Medical Oncology (2023) 40:318
https://doi.org/10.1007/s12032-023-02181-9

ORIGINAL PAPER

Synergistic induction of apoptosis in liver cancer cells: exploring the combined potential of doxorubicin and XL-888

Özlem Kaplan[1]

Received: 14 August 2023 / Accepted: 2 September 2023 / Published online: 4 October 2023

Abstract

Combination therapy has been frequently preferred in treating various types of cancer in recent years. Targeted cancer therapy has also become one of the remarkable treatment modalities. Therefore, the aim of the study to investigate its cytotoxic and apoptotic effects on liver cancer cell lines by combining the classical chemotherapeutic drug doxorubicin (DOX) and a targeted agent, the new generation HSP90 inhibitor XL-888. The molecular docking method was used to predict the binding conformation of XL-888 on the human Hsp90. The single and combined cytotoxic effects of DOX and XL-888 on liver cancer cell lines HepG2 and HUH-7 were determined by MTT assay. The effect of the combined use of two drugs was evaluated using Chou and Talalay method. The levels of apoptotic genes and heat shock proteins gene and protein expression levels were investigated by quantitative real-time polymerase chain reaction and western blotting, respectively. Molecular docking results showed that XL-888 selectively binds to the ATP binding pocket of HSP90 with an estimated free binding energy of − 7.8 kcal/mol. DOX and XL-888 and their combination showed dose-dependent cytotoxic effect. The combination of drugs showed a synergistic effect on both cell lines. The results revealed that the combination of DOX and XL-888 potently induced apoptosis in liver cancer cell lines rather than using drugs alone. The combined treatment of DOX and XL-888 demonstrated synergistic cytotoxic and apoptotic effects on liver cancer cell lines, presenting a promising approach for combination therapy in liver cancer.

Keywords HSP90 inhibition · Combination treatment · Doxorubicin · XL-888 · Liver cancer

Introduction

Liver cancer ranks among the top five most prevalent cancers worldwide, posing a significant global health burden. Hepatocellular carcinoma (HCC) represents the majority (85%) of liver cancer cases and is associated with a dismal prognosis primarily attributed to delayed diagnosis and limited therapeutic interventions [1]. There are usually no symptoms in the early stages of HCC, and symptoms appear in the later stages [2]. Radiofrequency ablation, surgical excision, transplantation, and transarterial chemoembolization are frequent therapy choices. HCC treatment is complicated by drug resistance and unwanted effects. As a result, these therapeutic techniques have a high rate of recurrence and a low probability of survival [3].

DOX is the most often utilized anticancer drug in HCC chemotherapy. DOX is also one of the first anticancer medicines to be employed in the treatment of liver cancer [4]. DOX has anticancer activity through penetrating the DNA helix and/or covalently attaching to DNA replication and transcription proteins. DOX causes cell death by inhibiting DNA, RNA, and protein synthesis [5]. DOX treatment causes cellular damage that affects not just cancer cells but also healthy cells, slowing or stopping their proliferation [6]. Furthermore, the use of DOX in treatment causes cardiotoxicity by increasing oxidative stress, which affects the heart tissue and causes cardiomyopathy [7]. The most typical cancer treatment method is to use a combination of medications to enhance the anticancer efficacy of existing drugs while lowering their undesirable side effects [8, 9]. Due to the intricate nature of HCC, concentrating solely on a single signaling pathway component may prove ineffective. Therefore, an ideal molecular target is one that can simultaneously

✉ Özlem Kaplan
ozlem.kaplan@alanya.edu.tr

[1] Department of Genetics and Bioengineering, Rafet Kayış Faculty of Engineering, Alanya Alaaddin Keykubat University, Antalya, Turkey

modify multiple components within one or more signaling pathways.

Heat shock protein 90 (HSP90) emerges as a particularly compelling candidate in this regard. HSP90 is a vital molecular chaperone known to interact with numerous client proteins, numbering in the hundreds [10]. Its significance lies in its ability to regulate the folding, stability, and activity of these client proteins, thereby exerting a substantial influence on various signaling pathways implicated in HCC. By targeting HSP90, it becomes possible to modulate multiple components simultaneously, potentially leading to more effective therapeutic strategies for HCC [11]. HSP90 regulates a wide range of oncoproteins' stability, function, and activity. These proteins are rapidly destroyed by the proteasome in the absence of HSP90 [12]. Because many of these proteins are frequently dysregulated in HCC, HSP90 may be a promising therapeutic target [13]. HSP90 has recently been identified as a possible HCC biomarker, with its expression having diagnostic relevance for HCC diagnosis [14].

Several highly selective but chemically different HSP90 inhibitors have been demonstrated to have potent anticancer efficacy [15, 16]. Among the numerous HSP90 inhibitors, XL-888, a next-generation oral drug targeting HSP90, has been shown to significantly limit HSP90 activity without inhibiting other kinases [17]. While preclinical trials of XL-888 in melanoma and advanced pancreatic/colorectal cancer are ongoing, there are insufficient studies on its biological significance in liver cancer [18, 19].

In this regard, we investigated the efficiency of combining the commonly used genotoxic drug DOX with the HSP90 inhibitor XL-888 to utilize various stress signaling pathways for cancer therapy. Also, it was demonstrated by molecular docking study that XL-888 selectively binds to the ATP binding pocket of HSP90 N-terminal domain (NTD). The Chou-Talalay method was used to compute the combination index (CI). When two drugs alone and as a combination, the effect on apoptotic genes and HSP genes were investigated with quantitative real-time polymerase chain reaction (qRT-PCR) and western blotting.

Materials and methods

Chemicals and reagents

XL-888 was purchased from AdooQ® Bioscience. Doxorubicin HCI was obtained by Gold Biotechnology Incorporated, USA. 3-(4,5dimethylthiazol-2-yl)-2,5-diphenyltetrazolium bromide (MTT), BCA protein assay kit, and RIPA lysis buffer were supplied from Serva. Polyvinylidene difluoride (PVDF) membrane (741260) was from Macherey-Nagel. Anti-HSP27 (ab5579), anti-HSP70 (ab79852), anti-HSP90 (ab2928), Anti-Bax (ab53154), Anti-Bcl-2 (ab59348), and goat anti-rabbit IgG H&L (HRP) (ab205718) antibodies were purchased from Abcam. Anti-pro-Casp-9 (M00080-1) antibody was purchased from Boster Bio. Anti-GAPDH (10494-1-AP) antibody was purchased from Proteintech. Primers were synthesized from Metabiomics. SYBR Green master mix was from Bioline. The total RNA isolation kit was from Favorgen Biotech Corp. cDNA synthesis cDNA synthesis kits were supplied from Bio-Rad. The enhanced chemiluminescence (ECL) substrate kit (1705060) was from Bio-Rad. Dulbecco's Modified Eagle's medium (DMEM) High Glucose, fetal bovine serum (FBS heat-inactivated), penicillin–streptomycin solution, L-glutamine, phosphate buffer saline (PBS), and trypsin–EDTA was purchased from Biological Industries. HepG2 and HUH-7 cell lines were from ATCC (American Type Culture Collection).

Molecular docking

The 3D structure of the target protein HSP90 NTD was obtained from the Protein Data Bank (PDB), while the molecular structure of XL-888 was sourced from the NCBI PubChem database. The HSP90 protein construct was found in a complex with ATP (PDB ID: 3T0Z). The downloaded complex has a resolution of 2.19 Å. Complex and imaged with XL-888 Chimera 1.16. ATP was removed from the complex before preparing the HSP90 NTD docking. HSP90 protein and XL-888 molecule were prepared for docking using Chimera 1.16 DocPrep tool. To identify the potential interaction site between the target protein and the ligand, a grid box was created by AutoDock Vina. The grid box had specific coordinates in the x, y, and z dimensions, namely 9.63, − 5.88, and 16.34, respectively. Its size was set to $22 \times 22 \times 22$. The docking procedure was conducted using Autodock Vina, and upon completion of the analyses, Biovia Discovery Studio was employed to visualize the interactions between the ligand and the active site residues of the target protein.

Cell culture

HepG2 and HUH-7 cancer cell lines were cultured in DMEM High Glucose medium supplemented with 0.1% penicillin–streptomycin, 1% L-glutamine, and 10% FBS. The cancer cell lines were incubated at 37 °C in a humid environment containing 5% CO_2.

Cell viability assay

The in vitro cytotoxic effect of XL-888 and DOX was determined by the MTT assay. The cancer cells were grown in 96-well culture plates (5×10^4 cells per well) and treated with XL-888 and DOX at concentrations ranging from 100 to 1.56 and 25 to 0.39 nM for 48 h, respectively.

Individual cytotoxicity assays of drugs were studied in serial dilutions with maximum initial concentrations of 100 nM for DOX and 25 nM for XL-888. In combination studies, considering the individual cytotoxicity values of the drugs, the ratio of 100 nM: 25 nM, i.e., 4:1, was studied and serial dilution was made by keeping this ratio constant. Following the incubation period, 100 µL of MTT solution (5 mg/mL) was added to each well and incubated at 37 °C for 3 h. The formazan product was then dissolved in 100 µL of dimethyl sulfoxide after MTT was removed. The absorbance was measured at 570 nm by a microplate reader, and the viability of cancer cells was calculated as a percentage of the control group.

Quantitative RT-PCR

The expression levels of *HSP27*, *HSP70*, *HSP90*, *Bax*, *Bcl-2*, *Cas-9*, *P53*, and *Cyt C* genes in HepG2 and HUH-7 cells treated with XL-888 and DOX, compared to untreated cells, were analyzed using RT-PCR (Bio-Rad CFX96TM). The primers used for the amplification of these genes were listed in Table 1. HepG2 and HUH-7 cells were treated with IC_{50} doses of XL-888 and DOX for 48 h. After the incubation period, total RNA was extracted from the cells, and cDNA synthesis was performed following the instructions provided in the kit. The RT-PCR was carried out as described in a previous method [20]. The expression levels of the genes were analyzed by the $2^{-\Delta\Delta Ct}$ method. The GAPDH gene was used as a reference or housekeeping gene for normalization.

Table 1 The primer sequences of genes (F: Forward, R: Reverse)

Bax	F	5′-TCAGGATGCGTCCACCAAGAAG-3′
	R	5′-TGTGTCCACGGCGGCAATCATC-3′
Bcl-2	F	5′-ATCGCCCTGTGGATGACTGAGT-3′
	R	5′-GCCAGGAGAAATCAAACAGAGGC-3′
Cas-9	F	5′-GTTTGAGGACCTTCGACCAGCT-3′
	R	5′-CAACGTACCAGGAGCCACTCTT-3′
P53	F	5′-CCTCAGCATCTTATCCGAGTGG-3′
	R	5′-TGGATGGTGGTACAGTCAGAGC-3′
Cyt C	F	5′CGTTGTGCCAGCGACTAAAAA-3′
	R	5′-GATTTGGCCCAGTCTTGTGC-3′
Hsp27	F	5′-CTGACGGTCAAGACCAAGGATG-3′
	R	5′-GTGTATTTCCGCGTGAAGCACC-3′
Hsp70	F	5′-ACCTTCGACGTGTCCATCCTGA-3′
	R	5′-TCCTCCACGAAGTGGTTCACCA-3′
Hsp90	F	5′-TCTGCCTCTGGTGATGAGATGG-3′
	R	5′-CGTTCCACAAAGGCTGAGTTAGC-3′
Gapdh	F	5′-GTCTCCTCTGACTTCAACAGCG-3′
	R	5′-ACCACCCTGTTGCTGTAGCCAA-3′

Western blotting

Western blot was used to investigate the protein expression levels of HSP27, HSP70, HSP90, BAX, BCL-2, and CAS-9 in cells exposed to XL-888 and DOX. The cells were treated with IC_{50} concentrations of XL-888 and DOX for 48 h. After incubation, cells were harvested with trypsin and lysed with RIPA buffer. Western blotting was performed as detailed previously [21]. Anti-HSP27 (1:1000), anti-HSP70 (1:500), and anti-HSP90 (1:500) were used as primary antibodies. Goat anti-rabbit IgG H&L (HRP) (1:10,000) was used as the secondary antibody. The protein bands were then observed using the ChemiDocTM imaging system (Bio-Rad) and an enhanced chemiluminescence (ECL) substrate. ImageLab 6.1 software was used to determine the levels of protein expression.

Statistical analysis

Statistical analysis and comparable data sets were evaluated with a two-way ANOVA with Sidak test and Dunnett's test using GraphPad Prism 8.0 software. Statistical significance was defined as $p < 0.05$ probability values. To study the synergistic efficacy of the drug combination, the Chou-Talalay approach was used to calculate the CI by CompuSyn software version 1.0.

Results and discussion

Molecular docking method was used to predict the binding conformation on human Hsp90 NTD, aiming to gain information about the potential anticancer effects of XL-888. The in-silico analysis demonstrated that XL-888 displayed a specific affinity for the conserved ATP binding pocket. Remarkably, it exhibited a significant binding energy of − 7.8 kcal/mol (Fig. 1A), emphasizing its potential as a promising candidate for anticancer therapy. It was determined that there is a Van der Waals interaction with Ser42, the Gly122 and Thr174 residues of the HSP90 protein form carbon-hydrogen bonds with the XL-888 molecule. Also, pi-Sulfur (Met88), amide-pi stacked (Asn41), alkyl (Phe128, Val140, Leu38, Leu97, Val176) and pi alkyl (Ala45) were calculated as possible hydrophobic interactions between HSP90 and XL-888 molecule (Fig. 1B, C). The interactions and bond distances between HSP90 NTD and XL-888 molecule are shown in Table 2.

Liver cancer cell lines HepG2 and HUH-7 were used to determine the effects of DOX and HSP90 inhibitor XL-888 on human liver cancer cell viability. In liver cancer research, HepG2 and HUH-7 cells are considered the gold standard and widely recognized as representative models of liver cancer. These cell lines typically mirror the characteristics

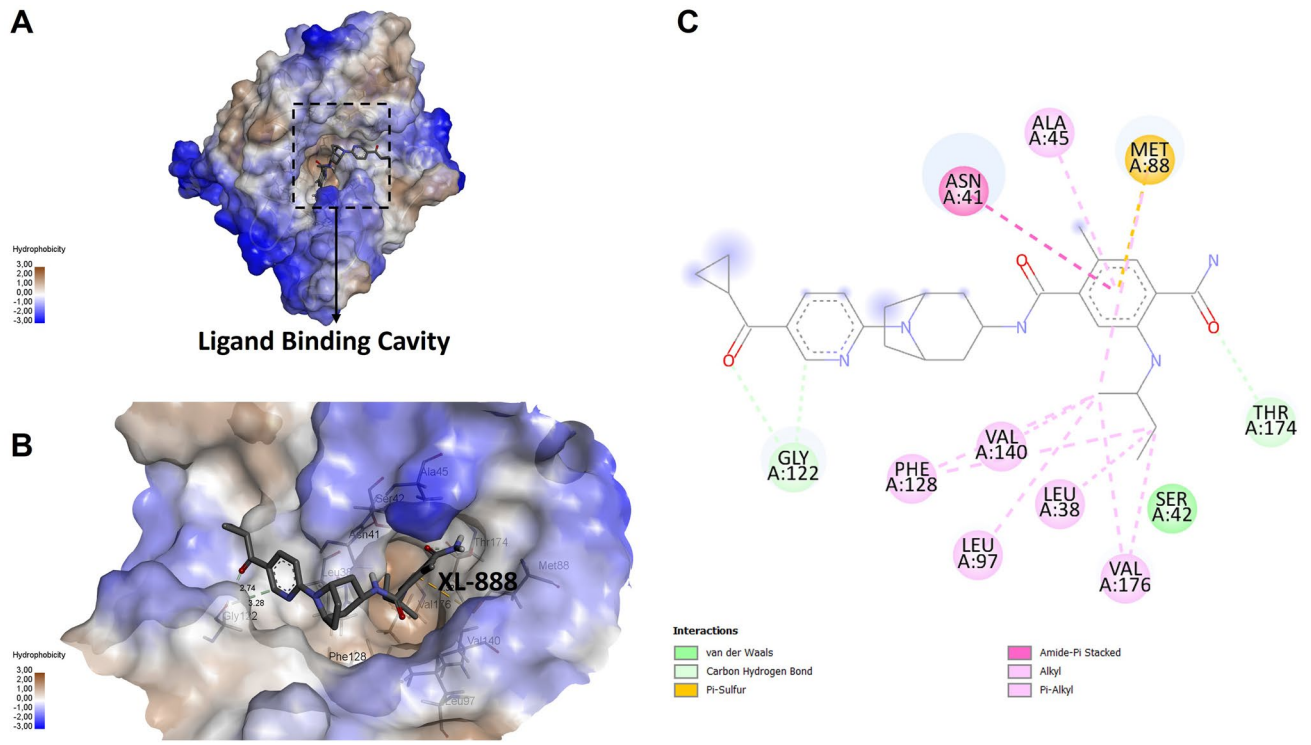

Fig. 1 **A** Binding sites of XL-888 on the human Hsp90 NTD. **B** Key residues involved in the interaction between Hsp90 NTD and XL-888. **C** 2D representation illustrating the interaction surface of XL-888 and Hsp90 protein

Table 2 Molecular docking interactions and bond distances of XL-888 with HSP90 protein

Residue	Distance (Å)	Bound catagory	Bound types
Gly122	2.74	Hydrogen bond	Carbon hydrogen bond
Thr174	2.83	Hydrogen bond	Carbon hydrogen bond
Gly122	3.28	Hydrogen bond	Carbon hydrogen bond
Met88	4.32	Other	Pi–sulfur
Asn41	5.40	Hydrophobic	Amide–Pi stacked
Met88	5.41	Hydrophobic	Alkyl
Leu97	4.80	Hydrophobic	Alkyl
Val140	4.29	Hydrophobic	Alkyl
Val176	4.81	Hydrophobic	Alkyl
Leu38	4.80	Hydrophobic	Alkyl
Val176	4.24	Hydrophobic	Alkyl
Phe128	4.65	Hydrophobic	Pi–alkyl
Phe128	5.28	Hydrophobic	Pi–alkyl
Ala45	5.20	Hydrophobic	Pi–alkyl

observed in liver cancer and encompass the molecular attributes of this cancer type [22]. Hence, these cell lines were chosen for our study due to their well-established reputation in accurately reflecting the features of liver cancer. The effect of DOX and XL-888 on the cell viability in 48 h as a single agent and combination was determined by the MTT experiment. As shown in Fig. 2A and B, DOX and XL-888 exhibited dose-dependent inhibition in HepG2 and HUH-7 cell viability. The half maximal inhibitory concentration (IC_{50}) was 17 nM (DOX) and 5.32 nM (XL-888) in HepG2 cells, while 10.58 nM (DOX) and 4.28 nM (XL-888) in HUH-7 cells. The HUH-7 cells were relatively more sensitive to these two drugs. In addition, the XL-888 and DOX combination had a stronger inhibitor effect than use as an agent alone on HepG2 and HUH-7 cell viability (Fig. 3A, B).

These data suggest that the XL-888 and DOX combination may be synergistic to inhibit cell viability in liver cancer cells. To verify this synergism, we treated the cells with a combination of two agents at a constant rate. We used the CompuSyn software to calculate the CI as described under Chou and Talalay's methods [23]. The analysis reveals that the combination effects of two agents can be summarized in the following manner: when CI is less than 1, it indicates synergistic effects; when CI equals 1, it signifies additional effects; and when CI is greater than 1, it denotes antagonistic effects [24]. XL-888 and DOX combination tested liver cancer cells HepG2 (Fig. 3C), and HUH-7 (Fig. 3D) showed synergistic anticancer activity.

We analyzed the effect of DOX and XL-888 (individually and in combination) on apoptotic and HSPs on liver cancer cell lines by qRT-PCR and Western Blot experiments

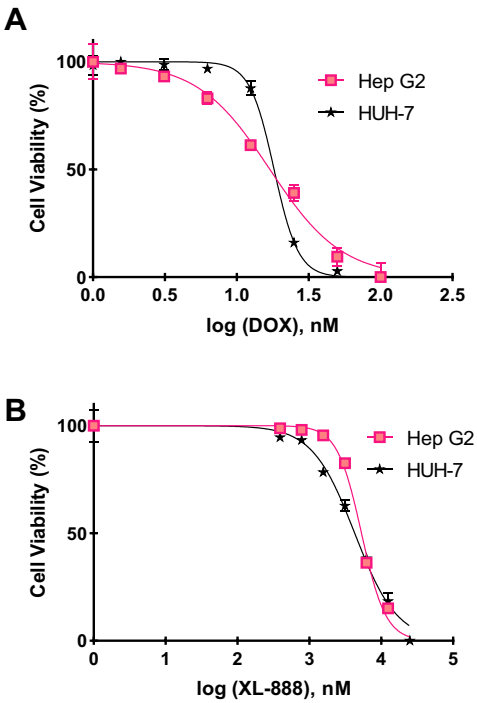

IC_{50} (nM)	
HepG2	HUH-7
17.00 ± 0.0005	10.58 ±0.0003

IC_{50} (nM)	
HepG2	HUH-7
5.32± 0.0002	4.28 ±0.0004

Fig. 2 Cytotoxic effect and IC_{50} values of DOX (**A**) and XL-888 (**B**) in HepG2 and HUH-7 cells at 48 h

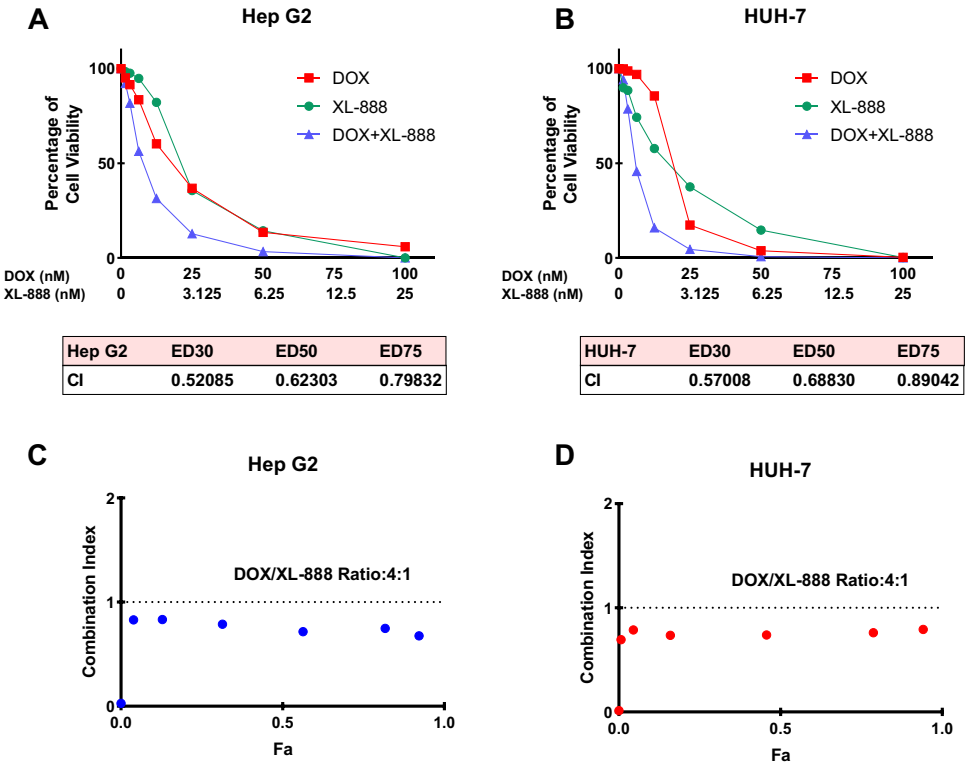

Hep G2	ED30	ED50	ED75
CI	0.52085	0.62303	0.79832

HUH-7	ED30	ED50	ED75
CI	0.57008	0.68830	0.89042

Fig. 3 Cytotoxic effect of DOX and XL-888 combination in HepG2 (**A**) and HUH-7 (**B**) cancer cell lines and fraction affected (Fa) versus CI plots obtained from median-effect analysis of Chou–Talalay for HepG2 (**C**) and HUH-7 (**D**) cancer cell lines. **Fa* fraction affected, *CI* combination index, ED30, ED50, and ED75 refer to the doses at which 30%, 50%, and 75% of cells or organisms are effectively inhibited, respectively. These values provide insights into the potency of a drug or treatment, demonstrating its ability to achieve desired outcomes at specific dosage levels

to investigate the synergistic mechanism of drug combination. The effect of DOX and XL-888, which was applied to liver cancer cell series as a single agent and combination, on apoptotic genes and HSP genes was investigated with RT-PCR (Figs. 4A and 5A). When HSP90 activity was inactivated with XL-888, a significant increase was observed in the *Bax/Bcl-2* ratio in HepG2 and HUH-7 cell lines, while there was no significant change in *Cas-9* and *Cyt C* gene expression levels. However, expression of the *p53* gene increased in HepG2 cells, while a significant decrease

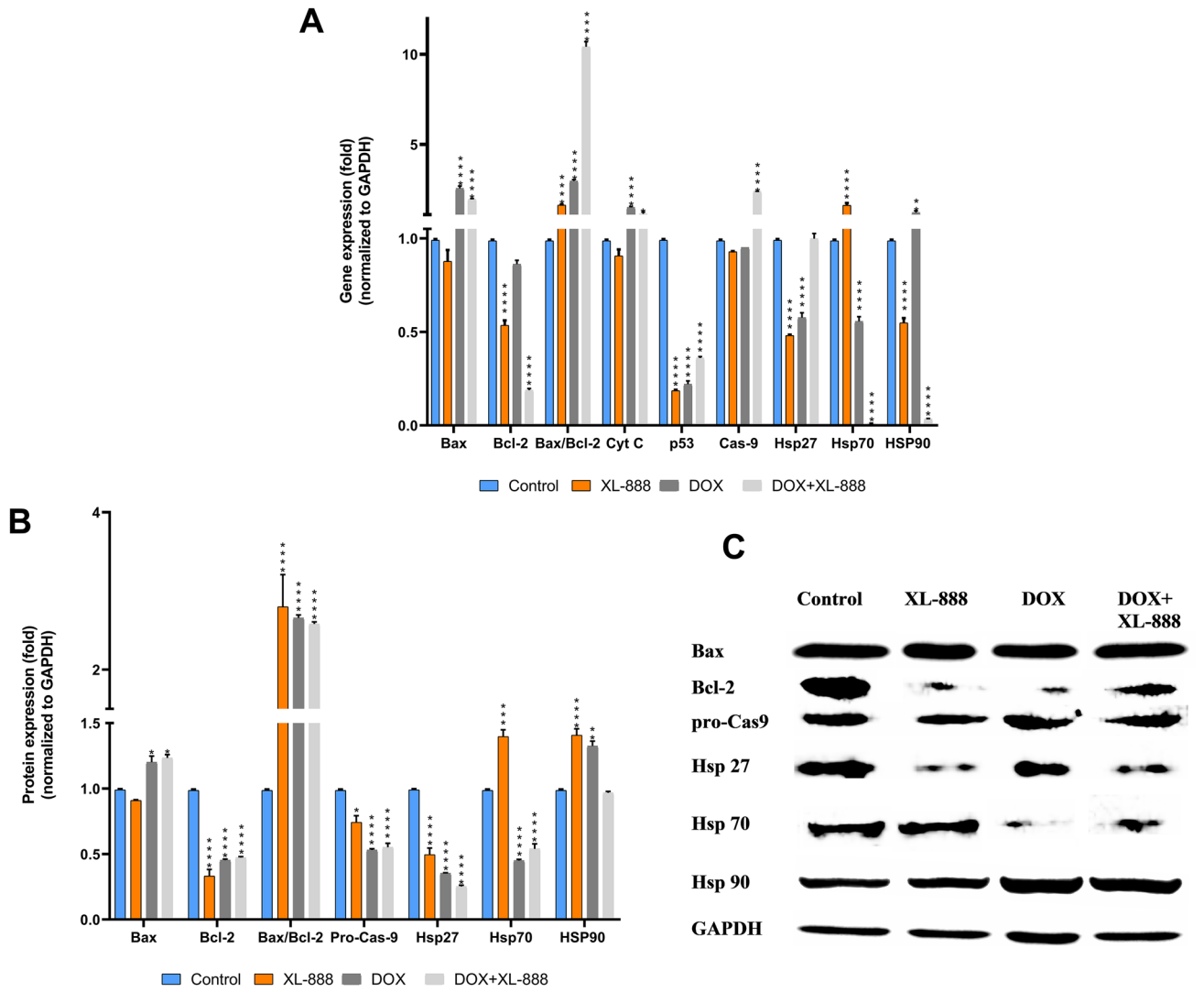

Fig. 4 Analysis of changes in the expressions of apoptotic genes (*Bax*, *Bcl-2*, *Cyt C*, *p53*, *Cas-9*) and HSP genes (*HSP27*, *HSP70*, *HSP90*) following a 48 h treatment with XL-888, DOX, and DOX + XL-888 in HUH-7 cells. **A** Focuses on alterations in gene expressions, while **B** highlights changes in protein expressions of apoptotic markers (Bax, Bcl-2, pro-Cas-9) and HSPs (HSP27, HSP70, HSP90). **C** summarizes the abundance of apoptotic and HSPs in HUH-7 cell lines. The data are represented as the mean ± SEM (n = 3). Statistical significance is denoted as *p < 0.05, **p < 0.01, ***p < 0.001, and ****p < 0.0001 when compared to the control group

was observed in *p53* gene expression in HUH-7 cells. This may be due to different p53 states in the two cell lines. The tumor suppressor protein p53, which is mutated in over 50% of human cancers, is a significant client protein of HSP90. Previous studies have indicated that inhibition of HSP90 can lead to the ubiquitination and degradation of mutant p53 through the proteasome pathway. Blocking HSP90 activity in this manner induces apoptosis in a manner that is dependent on the presence of functional p53 [25]. In our study, it is thought that XL-888 treatment triggered the downregulation of mutant p53 protein in HUH-7 cells while promoting upregulation of wild-type p53 expression in HepG2 cells, thereby activating the apoptotic pathway.

Inhibition of *HSP90* activity resulted in *HSP70* upregulation in both liver cancer cell lines. This effect may be due to the dissociation of heat shock factor 1 (HSF1) monomer from HSP90, followed by HSF1 trimerization, nuclear translocation, and transcriptional activation of HSP70, as clearly stated in previous studies [26, 27]. When *HSP27* and *HSP90* gene levels were examined, there was no significant change in HepG2, but a dramatic decrease was observed in HUH-7 cells. The findings of this study indicate that the response of each cell line to XL-888 treatment is distinct. *HSP27* appears to play a cytoprotective role by directly inhibiting cell apoptosis through its interaction with crucial proteins involved in apoptotic pathways. Additionally, HSP27 can

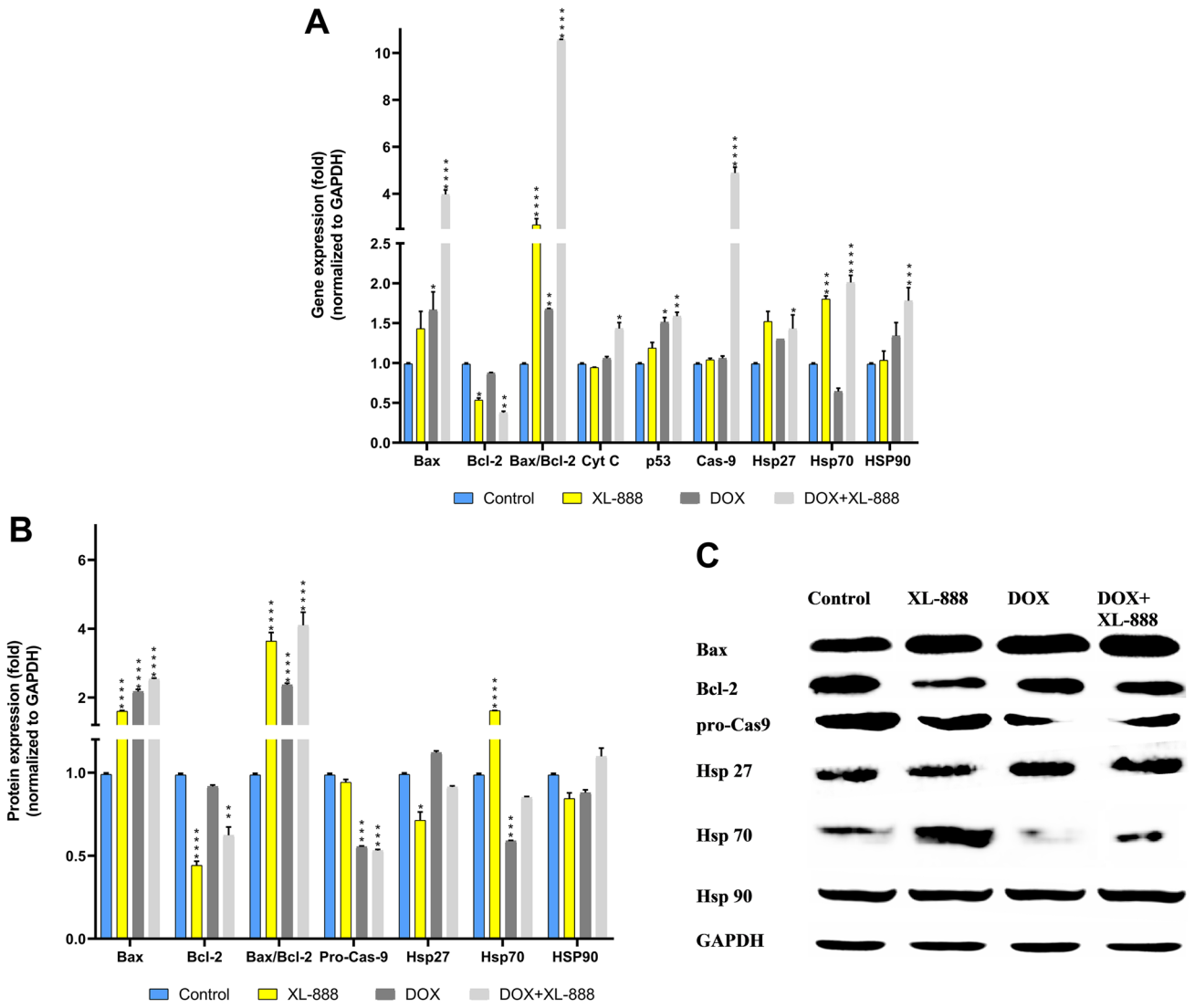

Fig. 5 Analysis of changes in the expressions of apoptotic genes (*Bax*, *Bcl-2*, *Cyt C*, *p53*, *Cas-9*) and HSP genes (*HSP27*, *HSP70*, *HSP90*) following a 48 h treatment with XL-888, DOX, and DOX + XL-888 in HepG2 cells. **A** Focuses on alterations in gene expressions, while **B** highlights changes in protein expressions of apoptotic markers (Bax, Bcl-2, pro-Cas-9) and HSPs (HSP27, HSP70, HSP90). **C** The abundance of apoptotic and HSPs in HepG2 cell lines. The data are represented as the mean ± SEM (n = 3). Statistical significance is denoted as *p < 0.05, **p < 0.01, ***p < 0.001, and ****p < 0.0001 when compared to the control group

enhance cell survival by modulating the phosphorylation of ERK and Akt signaling pathways, as well as facilitating the degradation of components associated with apoptosis. These observations highlight the multifaceted mechanisms through which *HSP27* influences cell fate and underscore its potential as a therapeutic target in cancer treatment. In HCC, downregulation of *HSP27* has been reported to induce obvious cell apoptosis [28].

When gene expression levels in cells treated with DOX were analyzed, there was an increase in *Bax/Bcl-2* ratio, *Cyt C*, and *Cas-9* levels in both cell lines. Like XL-888, the *p53* level increased in HepG2 cells and decreased in HUH-7 cells. DOX caused a decrease in the HSP70 gene expression level and increased the HSP90 gene expression level in both cell lines.

When XL-888 and DOX were administered together, the increase in *Bax/Bcl-2* ratio in HepG2 and HUH-7 cell lines was higher than when drugs were administered alone. Similarly, combined drug administration in both cell lines showed a significant increase in *Cyt C* and *Cas-9* gene expressions. *p53* gene expression showed a similar pattern, increasing in HepG2 cells and decreasing in HUH-7 cells. When HSP expressions were examined, the combination caused an increase in *HSP27*, *HSP70*, and *HSP90* gene expressions in HepG2 cells, while *HSP70* and *HSP90*

expression decreased in HUH-7 cells, but there was no significant change in *HSP27* expression.

In the HepG2 and HUH-7 cells, where two drugs are applied alone and as a combination, the change in the expressions of apoptotic protein and HSP proteins was analyzed with Western Blotting (Figs. 4B, C, 5B, C).

In HepG2 and HUH-7 cells, where XL-888 inhibited the HSP90 protein, an increase in Bax/Bcl-2 ratios and a decrease in pro-Cas-9 levels revealed that the cells exhibited an apoptotic profile. These results were parallel to the RT-PCR results. In general, although the change in the protein level of HSP supported the RT-PCR results, it resulted in a significant increase in the protein level despite a decrease in the HSP90 gene expression level in HUH-7 cells. The change in expression levels of apoptotic proteins in both cell lines after DOX treatment was similar to that of XL-888. The change in the level of HSP proteins was not different from the change in gene expression levels.

The combination of XL-888 and DOX caused an apoptotic cell profile because of the increase in Bax/Bcl-2 and a decrease in pro-Cas-9 levels in both cell lines. In the expression of HSP proteins, the combination of the two drugs resulted in a decrease in Hsp27 and HSP70 levels and no change in HSP90 protein levels. The data presented in this study indicate that the drug combination can activate caspases, which are key enzymes involved in the initiation and execution of apoptotic cell death. Apoptosis, known as programmed cell death, is the main way to evaluate the response to cytotoxic and tumor cell damage. The expression levels of pro-apoptotic (like Bax) and anti-apoptotic proteins (like Bcl-2) provide information about the apoptotic profile of cells. The release of cytochrome-c in the apoptotic process is regulated by pro-apoptotic and anti-apoptotic proteins. cytochrome-c, pro-cas-9, and APAF-1 forms an apoptosome complex and Cas-9 is activated via a proteolytic cleavage. The cleavaged Cas-9 activates the caspase 3 and caspase-7 for induction of the internal apoptotic cell death mechanisms in the cells. Therefore, increase of the Bax/Bcl-2 expression ratio and reducing the pro-Cas-9 protein levels are vital biomarkers to stimulate apoptosis in cancer cells and show the induction of apoptosis [29].

Given the complexity of liver cancer, as with many cancer cells, targeting a single component of a signaling pathway may be ineffective. Combining cancer drugs that possess distinct mechanisms of action represents a viable strategy to enhance therapeutic efficacy while minimizing undesirable side effects [30]. Within this framework, the concurrent administration of DOX with other cancer drugs has been extensively investigated in numerous studies. These investigations have demonstrated synergistic enhancements in cancer-specific toxicity while mitigating the risk of cardiotoxic side effects. By combining DOX with other agents, the therapeutic outcome can be significantly improved, offering a more effective and safer treatment approach for cancer patients. Daunys et al. showed that the HSP90 inhibitors ICPD47 and ICPD62, combined with DOX, can act synergistically on pancreatic cancer cells [31]. In another study, 17-AAG, an HSP90 inhibitor, sensitized breast cancer cells to the cytotoxic effects of DOX. Subsequently, Gupta et al. developed folate receptor-targeted hybrid lipid-core nanocapsules containing 17-AAG and DOX. These nanoparticles significantly inhibited the growth of MCF-7 cells via apoptosis [32]. In a study with an HSP90 inhibitor (ganetespib) and DOX, the combination of ganetespib and DOX showed significant synergy and was effective in inhibiting small cell lung cancer growth in vitro and in mouse xenograft models [33]. Drug combination studies can realize the full potential of the anticancer activity of individual drugs and expand the application of drugs to various types of cancer.

Administration of XL-888 alone and in combination has been investigated in various types of cancer. Zhang et al. investigated the use of Hsp90 inhibition by XL-888 to enhance the response to PD-1 blockade in pancreatic ductal adenocarcinoma. Their findings showed that XL-888 attenuates inflammatory signals and directly affects PDAC-associated cells, leading to improved immune responses in mouse models, and is a promising strategy for PDAC immunotherapy [18]. In a phase 1 clinical trial, the combination of XL-888 and pembrolizumab in patients with gastrointestinal adenocarcinoma had an acceptable safety profile and provided a long-term stable disease state in some patients, suggesting that this treatment may be a promising option for Phase 2 trials [34]. Studies are ongoing for this combination in colorectal and pancreatic cancer (NCT03095781). Two clinical studies on the use of XL-888 in melanoma cancer have been completed. The first includes a Phase I/II trial using vemurafenib and XL-888 in patients with BRAF-mutant melanoma, with a response rate of 75% of treated patients. The second is a Phase I trial of a triple regimen of dabrafenib, trametinib, and AT13387 in patients with BRAF-mutant solid tumors [35, 36].

In this particular study, our focus was on examining the toxic effects of combining DOX and XL-888 in liver cancer cells, as well as their potential to induce apoptosis. While XL-888 is currently undergoing preclinical trials for melanoma, advanced pancreatic cancer, and colorectal cancer, a recent study has also investigated its effects in HCC. Sun et al. conducted a study to explore the pro-apoptotic impact of XL-888 on HCC cells when combined with non-lethal heat treatment. To assess whether the combination of heat treatment with or without XL-888 induces apoptosis in HCC cell lines, the levels of caspase 3 and PARP cleavage were measured. The results demonstrated that both heat treatment and XL-888 treatment alone increased the levels of cleaved caspase 3 and PARP. Interestingly, combining the two treatments resulted in even higher levels of cleavage. These findings indicate that

the combination of XL-888 with heat treatment significantly enhances apoptosis in HCC cells [37]. In our study, DOX and XL-888 individually induced cellular death in liver cancer cell lines by inducing apoptosis, while the combination of the drug significantly increased apoptotic cell death compared to their use alone. In summary, our findings show the amazing synergistic impact found when DOX and XL-888 were combined in liver cancer cell lines, notably HepG2 and HUH-7. This combination therapy excelled individual pharmacological treatments in terms of effectiveness, potentially presenting a way to reduce the dose-dependent adverse effects associated with these drugs. The data given in this study provide a solid platform for future research into combination cancer therapy. The observed synergistic effects provide novel opportunities for more effective anticancer therapies in future treatments.

Conclusion

In this study, we demonstrated the synergistic effect of DOX and XL-888 on liver cancer cell lines on HepG2 and HUH-7. When used in combination, the drugs were more effective than they use it alone. Combined use of drugs is more effective than usage alone and may reduce the dose-dependent side effects of the drug. The data obtained in our study contain the first results for the use of DOX and XL-888 in liver cancer cells and may form the basis for future combined cancer therapy studies. The synergistic effect results are a promising avenue for more efficient anticancer treatments in future treatment strategies.

Acknowledgements The author would like to thank Prof. Dr. İsa Gökçe and Dr. Nazan Gökşen Tosun for contributions.

Author contributions ÖK: Investigation, methodology, formal analysis, writing—review and editing, visualization, methodology, resources.

Funding No support was received in this study. However, the facilities of Tokat Gaziosmanpasa University, Faculty of Engineering and Architecture, Department of Bioengineering laboratories were used.

Data availability Data and materials are available from the author upon request.

Declarations

Conflict of interest The author confirm that this article content has no conflicts of interest.

Ethical approval Not applicable.

References

1. Hajiasgharzadeh K, Somi MH, Shanehbandi D, Mokhtarzadeh A, Baradaran B. Small interfering RNA-mediated gene suppression as a therapeutic intervention in hepatocellular carcinoma. J Cell Physiol. 2019;234:3263–76. https://doi.org/10.1002/jcp.27015.
2. Chen S, Cao Q, Wen W, Wang H. Targeted therapy for hepatocellular carcinoma: challenges and opportunities. Cancer Lett. 2019;460:1–9. https://doi.org/10.1016/j.canlet.2019.114428.
3. Ferenci P, Fried M, Labrecque D, Bruix J, Sherman M, Omata M, et al. Hepatocellular carcinoma (HCC): a global perspective. J Clin Gastroenterol. 2010;44:239–45. https://doi.org/10.1097/MCG.0b013e3181d46ef2.
4. Le Grazie M, Biagini MR, Tarocchi M, Polvani S, Galli A. Chemotherapy for hepatocellular carcinoma: the present and the future. World J Hepatol. 2017;9:907–20. https://doi.org/10.4254/wjh.v9.i21.907.
5. Cagel M, Grotz E, Bernabeu E, Moretton MA, Chiappetta DA. Doxorubicin: nanotechnological overviews from bench to bedside. Drug Discovery Today. 2017;22:270–81. https://doi.org/10.1016/j.drudis.2016.11.005.
6. Radu ER, Semenescu A, Voicu SI. Recent advances in stimuli-responsive doxorubicin delivery systems for liver cancer therapy. Polymers. 2022;14:5249.
7. Mohammadi M, Arabi L, Alibolandi M. Doxorubicin-loaded composite nanogels for cancer treatment. J Control Release. 2020;328:171–91. https://doi.org/10.1016/j.jconrel.2020.08.033.
8. Yue W, Yupeng G, Jun C, Kui J. Apatinib combined with olaparib induces ferroptosis via a p53-dependent manner in ovarian cancer. J Cancer Res Clin Oncol. 2023;149:8681–9. https://doi.org/10.1007/s00432-023-04811-1.
9. Sturm M-J, Henao-Restrepo JA, Becker S, Proquitté H, Beck JF, Sonnemann J. Synergistic anticancer activity of combined ATR and ribonucleotide reductase inhibition in Ewing's sarcoma cells. J Cancer Res Clin Oncol. 2023;149:8605–17. https://doi.org/10.1007/s00432-023-04804-0.
10. Özgür A, Tutar Y. Heat shock protein 90 inhibition in cancer drug discovery: from chemistry to futural clinical applications. Anticancer Agents Med Chem. 2016;16:280–90. https://doi.org/10.2174/1871520615666150821093747.
11. Verma S, Goyal S, Jamal S, Singh A, Grover A. Hsp90: friends, clients and natural foes. Biochimie. 2016;127:227–40. https://doi.org/10.1016/j.biochi.2016.05.018.
12. Ren X, Li T, Zhang W, Yang X. Targeting heat-shock protein 90 in cancer: an update on combination therapy. Cells. 2022;11:2556.
13. Qin L, Huang H, Huang J, Wang G, Huang J, Wu X, et al. Biological characteristics of heat shock protein 90 in human liver cancer cells. Am J Transl Res. 2019;11:2477–83.
14. Wei W, Liu M, Ning S, Wei J, Zhong J, Li J, et al. Diagnostic value of plasma HSP90α levels for detection of hepatocellular carcinoma. BMC Cancer. 2020;20:6. https://doi.org/10.1186/s12885-019-6489-0.
15. Özgür A. Investigation of anticancer activities of STA-9090 (ganetespib) as a second generation HSP90 inhibitor in Saos-2 osteosarcoma cells. J Chemother. 2021;33:554–63. https://doi.org/10.1080/1120009X.2021.1908650.
16. Ozgur A, Tutar Y. Heat shock protein 90 inhibitors in oncology. Curr Proteomics. 2014;11:2–16.
17. Bussenius J, Blazey CM, Aay N, Anand NK, Arcalas A, Baik T, et al. Discovery of XL888: a novel tropane-derived small molecule inhibitor of HSP90. Bioorg Med Chem Lett. 2012;22:5396–404. https://doi.org/10.1016/j.bmcl.2012.07.052.
18. Zhang Y, Ware MB, Zaidi MY, Ruggieri AN, Olson BM, Komar H, et al. Heat shock protein-90 inhibition alters activation of pancreatic stellate cells and enhances the efficacy of PD-1 blockade in pancreatic cancer. Mol Cancer Ther. 2021;20:150–60. https://doi.org/10.1158/1535-7163.Mct-19-0911.
19. Vido MJ, Aplin AE. The broad stroke of Hsp90 inhibitors: painting over the RAF inhibitor paradox. J Investig Dermatol. 2015;135:2355–7. https://doi.org/10.1038/jid.2015.239.
20. Tosun NG, Kaplan Ö, Özgür A. Apoptosis induced by *Tarantula cubensis* crude venom (Theranekron® D6) in

cancer cells. Rev Bras. 2021;31:824–31. https://doi.org/10.1007/s43450-021-00221-x.
21. Kaplan Ö, Gökşen Tosun N, İmamoğlu R, Türkekul İ, Gökçe İ, Özgür A. Biosynthesis and characterization of silver nanoparticles from *Tricholoma ustale* and *Agaricus arvensis* extracts and investigation of their antimicrobial, cytotoxic, and apoptotic potentials. J Drug Deliv Sci Technol. 2022;69:103178. https://doi.org/10.1016/j.jddst.2022.103178.
22. Schicht G, Seidemann L, Haensel R, Seehofer D, Damm G. Critical investigation of the usability of hepatoma cell lines HepG2 and Huh7 as models for the metabolic representation of resectable hepatocellular carcinoma. Cancers (Basel). 2022. https://doi.org/10.3390/cancers14174227.
23. Chou T-C. Frequently asked questions in drug combinations and the mass-action law-based answers. Synergy. 2014;1:3–21. https://doi.org/10.1016/j.synres.2014.07.003.
24. Chou T-C. The combination index (CI < 1) as the definition of synergism and of synergy claims. Synergy. 2018;7:49–50. https://doi.org/10.1016/j.synres.2018.04.001.
25. Muller P, Hrstka R, Coomber D, Lane DP, Vojtesek B. Chaperone-dependent stabilization and degradation of p53 mutants. Oncogene. 2008;27:3371–83. https://doi.org/10.1038/sj.onc.1211010.
26. Trepel J, Mollapour M, Giaccone G, Neckers L. Targeting the dynamic HSP90 complex in cancer. Nat Rev Cancer. 2010;10:537–49. https://doi.org/10.1038/nrc2887.
27. Augello G, Emma MR, Cusimano A, Azzolina A, Mongiovì S, Puleio R, et al. Targeting HSP90 with the small molecule inhibitor AUY922 (luminespib) as a treatment strategy against hepatocellular carcinoma. Int J Cancer. 2019;144:2613–24. https://doi.org/10.1002/ijc.31963.
28. Wang C, Zhang Y, Guo K, Wang N, Jin H, Liu Y, et al. Heat shock proteins in hepatocellular carcinoma: molecular mechanism and therapeutic potential. Int J Cancer. 2016;138:1824–34. https://doi.org/10.1002/ijc.29723.
29. Ramalingam M, Jang S, Jeong HS. Therapeutic effects of conditioned medium of neural differentiated human bone marrow-derived stem cells on rotenone-induced alpha-synuclein aggregation and apoptosis. Stem Cells Int. 2021;2021:6658271. https://doi.org/10.1155/2021/6658271.
30. Anwanwan D, Singh SK, Singh S, Saikam V, Singh R. Challenges in liver cancer and possible treatment approaches. Biochim Biophys Acta Rev Cancer. 2020;1873:188314. https://doi.org/10.1016/j.bbcan.2019.188314.
31. Daunys S, Matulis D, Petrikaitė V. Synergistic activity of Hsp90 inhibitors and anticancer agents in pancreatic cancer cell cultures. Sci Rep. 2019;9:16177. https://doi.org/10.1038/s41598-019-52652-1.
32. Gupta B, Pathak S, Poudel BK, Regmi S, Ruttala HB, Gautam M, et al. Folate receptor-targeted hybrid lipid-core nanocapsules for sequential delivery of doxorubicin and tanespimycin. Colloids Surf B. 2017;155:83–92. https://doi.org/10.1016/j.colsurfb.2017.04.010.
33. Lai CH, Park KS, Lee DH, Alberobello AT, Raffeld M, Pierobon M, et al. HSP-90 inhibitor ganetespib is synergistic with doxorubicin in small cell lung cancer. Oncogene. 2014;33:4867–76. https://doi.org/10.1038/onc.2013.439.
34. Akce M, Alese OB, Shaib WL, Wu C, Lesinski GB, El-Rayes BF. Phase Ib trial of pembrolizumab and XL888 in patients with advanced gastrointestinal malignancies: results of the dose-escalation phase. J Clin Oncol. 2020;38:830–830. https://doi.org/10.1200/JCO.2020.38.4_suppl.830.
35. Eroglu Z, Chen YA, Gibney GT, Weber JS, Kudchadkar RR, Khushalani NI, et al. Combined BRAF and HSP90 inhibition in patients with unresectable BRAF V600E-mutant melanoma. Clin Cancer Res. 2018;24:5516–24.
36. Mooradian M, Cleary JM, Cohen JV, Lawrence DP, Buchbinder EI, Giobbie-Hurder A, et al. CTEP 9557: a dose-escalation trial of combination dabrafenib, trametinib, and AT13387 in patients with BRAF mutant solid tumors. J Clin Oncol. 2020;38(15_Suppl):3609.
37. Sun C, Bai M, Ke W, Wang X, Zhao X, Lu Z. The HSP90 inhibitor, XL888, enhanced cell apoptosis via downregulating STAT3 after insufficient radiofrequency ablation in hepatocellular carcinoma. Life Sci. 2021;282:119762. https://doi.org/10.1016/j.lfs.2021.119762.